AGU PUBLICATIONS

JGR

Journal of Geophysical Research: Space Physics

RESEARCH ARTICLE

10.1002/2017JA023975

Interactions between energetic electrons and realistic whistler mode waves in the Jovian magnetosphere

M. de Soria-Santacruz[1], Y. Y. Shprits[2,3], A. Drozdov[2], J. D. Menietti[4], H. B. Garrett[1], H. Zhu[2], A. C. Kellerman[2], and R. B. Horne[5]

[1]Jet Propulsion Laboratory, California Institute of Technology, Pasadena, California, USA, [2]Department of Earth, Planetary, and Space Sciences, University of California, Los Angeles, California, USA, [3]Helmholtz Centre Potsdam, GFZ German Research Centre for Geosciences, Potsdam, Germany, [4]Department of Physics and Astronomy, University of Iowa, Iowa City, Iowa, USA, [5]British Atlantic Survey, Cambridge, UK

Key Points:
- The contribution to the electron dynamics from upper band chorus waves is almost negligible compared to that from lower band chorus
- The competition between loss and acceleration mechanisms can be influenced by the latitudinal distribution of the waves
- The shape of the electron phase space density is important for both electron acceleration and loss

Correspondence to:
M. de Soria-Santacruz,
mpich@jpl.nasa.gov

Citation:
de Soria-Santacruz, M., Y. Y. Shprits, A. Drozdov, J. D. Menietti, H. B. Garrett, H. Zhu, A. C. Kellerman, and R. B. Horne (2017), Interactions between energetic electrons and realistic whistler mode waves in the Jovian magnetosphere, *J. Geophys. Res. Space Physics*, *122*, 5355–5364, doi:10.1002/2017JA023975.

Received 31 JAN 2017
Accepted 9 MAY 2017
Accepted article online 15 MAY 2017
Published online 23 MAY 2017

Abstract The role of plasma waves in shaping the intense Jovian radiation belts is not well understood. In this study we use a realistic wave model based on an extensive survey from the Plasma Wave Investigation on the Galileo spacecraft to calculate the effect of pitch angle and energy diffusion on Jovian energetic electrons due to upper and lower band chorus. Two Earth-based models, the Full Diffusion Code and the Versatile Electron Radiation Belt code, are adapted to the case of the Jovian magnetosphere and used to resolve the interaction between chorus and electrons at $L = 10$. We also present a study of the sensitivity to the latitudinal wave coverage and initial electron distribution. Our analysis shows that the contribution to the electron dynamics from upper band chorus is almost negligible compared to that from lower band chorus. For 100 keV electrons, we observe that diffusion leads to redistribution of particles toward lower pitch angles with some particle loss, which could indicate that radial diffusion or interchange instabilities are important. For energies above >500 keV, an initial electron distribution based on observations is only weakly affected by chorus waves. Ideally, we would require the initial electron phase space density before transport takes place to assess the importance of wave acceleration, but this is not available. It is clear from this study that the shape of the electron phase space density and the latitudinal extent of the waves are important for both electron acceleration and loss.

1. Introduction

The discovery of decimetric wavelength emissions (tens to hundreds of centimeters) [*Burke and Franklin*, 1955; *Drake and Hvatum*, 1959; *Radhakrishnan and Roberts*, 1960] was the first proof of the presence of relativistic electrons trapped in the magnetic field of Jupiter [e.g., *Carr and Gulkis*, 1969; *Berge and Gulkis*, 1976; *Bolton et al.*, 2002]. Synchrotron radiation from energetic trapped electrons peaking around 1.5 R_J is responsible for the observed emissions, and their long-term variation of months to years [*Gerard*, 1970, 1976; *Klein*, 1976, 1989] has been shown to be directly correlated to changes in the spatial distribution of these trapped energetic particles (the Jovian radiation belts) for $L < 4\,R_J$ [*De Pater*, 1981; *De Pater and Goertz*, 1990, 1994; *Dulk et al.*, 1999a, 1999b]. Losses due to synchrotron radiation are most important in the inner portion of the magnetosphere, and initial modeling efforts included this mechanism as well as radial diffusion and interaction with neutrals [*Santos-Costa and Bourdarie*, 2001; *Santos-Costa et al.*, 2008; *Sicard and Bourdarie*, 2004], but they left aside the effect of wave-particle interactions.

The radiation belts of Jupiter are the most intense of all the planets in the solar system [*Bolton et al.*, 2002]. Their source is not well understood, but they are believed to be the result of inward radial transport beyond the orbit of Io [*Santos-Costa and Bourdarie*, 2001; *Sicard and Bourdarie*, 2004]. *Divine and Garrett* [1983] provided an empirical model of the Jovian environment based on measurements from Pioneer and Voyager spacecraft, and data from synchrotron radiation were added to the model in a latter publication [*Garrett et al.*, 2005]. The Galileo Interim Radiation Electron (GIRE) model [*Garrett et al.*, 2002] and its updated version 2 (GIRE2) [*de Soria-Santacruz et al.*, 2016] incorporated data from the Galileo Energetic Particles Detector (EPD) [*Williams et al.*, 1992] to the data-starved model from *Divine and Garrett* [1983]. A separate modeling effort from the Office National d'Études et de Recherches Aérospatiales (ONERA) is the Jovian Specification Environment Model (JOSE) [*Sicard-Piet et al.*, 2011] that combines the physics-based theoretical model

in *Sicard and Bourdarie* [2004] with in situ data from the Galileo EPD. These models, however, do not characterize the effect of magnetospheric waves on the dynamics of the intense Jovian radiation belts, but diffusion simulations that include wave-particle interactions are needed to study this variability. In the case of Earth, the radiation belts are the result of local acceleration [e.g., *Summers et al.*, 1998; *Horne and Thorne*, 1998; *Shprits et al.*, 2006a] and radial diffusion [e.g., *Kellogg*, 1959; *Shprits and Thorne*, 2004] from whistler waves, and it has been suggested that this type of acceleration may also be significant in the magnetosphere of Jupiter [*Horne et al.*, 2008; *Shprits et al.*, 2012]. Different diffusion codes have been developed to study the dynamics of the Earth's magnetosphere and characterize the interaction between relativistic electrons and whistler waves. In the present paper we adapt one of these codes, the two-dimensional version of the Versatile Electron Radiation Belt (VERB) computer code [*Shprits et al.*, 2009; *Subbotin et al.*, 2010], to the case of the Jovian magnetosphere.

Exploratory two-dimensional studies exist based on preliminary wave measurements. *Horne et al.* [2008] were the first to use a basic model of whistler mode waves at Jupiter based on Galileo observations to estimate diffusion coefficients, and they showed that waves are strong enough to accelerate electrons to relativistic energies. In a later publication, *Shprits et al.* [2012] also used a basic whistler wave model to compare the effect of pitch angle and energy diffusion at Earth, Jupiter, and Saturn and studied the sensitivity to the assumed initial phase space density (PSD) and the theoretical latitudinal wave distribution. *Shprits et al.* [2012] confirmed that interactions with whistler waves are responsible for significant local acceleration of electrons at Jupiter and suggested that the latitudinal distribution of the waves has a determining role in the dynamics of energetic electrons. Similarly, *Woodfield et al.* [2013, 2014] continued studying the interaction between chorus waves and energetic electrons using wave data from *Menietti et al.* [2008], which was based on preliminary measurements of whistler waves but it did not provide a complete survey of the wave data as a function of spatial parameters. In the present manuscript, we use realistic parameters to determine the importance of whistler emissions in the acceleration and loss of electrons in the Jovian magnetosphere. More specifically, we use the extensive wave survey from *Menietti et al.* [2016] and initial conditions derived from the GIRE2 empirical electron model to estimate the pitch angle and energy diffusion of the electron population due to lower and upper band chorus as a function of their latitude coverage. Finally, we study the sensitivity to the initial PSD by comparing the simulation results from the GIRE2 initial condition with those from a flat initial PSD as well as from the PSD used by *Shprits et al.* [2012]. The study focuses on the Jovian environment close to the orbit Europa but far away from the moon to avoid the introduction of any moon-induced effects. The region around Europa is of special interest to the heliophysics and planetary physics communities and also to engineers and spacecraft designers due to its connection to the planned Europa Clipper mission [*Jet Propulsion Laboratory*, 2017].

The paper is organized as follows: Section 2 describes the codes, input parameters, and models required to calculate diffusion coefficients and the evolution of the phase space density. Section 3 presents the results from the simulations, and section 4 concludes with a summary and discussion of the findings.

2. Models and Input Parameters

We use the VERB code to model electron flux and the timescale for electron acceleration in the Jovian magnetosphere. The code is based on a 3-D solution of the Fokker-Planck equation [*Schulz and Lanzerotti*, 1972] including radial, energy, pitch angle, and mixed diffusion terms. The present study, however, focuses on 2-D diffusion at $L = 10$ (where the L shell is the McIlwain parameter and it is the distance from the magnet to the dipole field line measured in Jupiter radii at the magnetic equator) including pitch angle, energy, and mixed diffusion terms using the implicit method from *Subbotin et al.* [2010]. The 2-D diffusion equation from can be written as follows:

$$\frac{\partial f}{\partial t} = \frac{1}{p^2}\frac{\partial}{\partial p}|_{y,L} p^2 \left(< D_{pp}(y,p) > \frac{\partial f}{\partial p}|_{y,L} + < D_{\alpha p}(y,p) > \frac{\partial f}{\partial y}|_{p,L} \right) + \frac{1}{T(y)y}\frac{\partial}{\partial y}|_{p,L} T(y) y \left(< D_{\alpha\alpha}(y,p) > \frac{\partial f}{\partial y}|_{p,L} + < D_{\alpha p}(y,p) > \frac{\partial f}{\partial p}|_{y,L} \right) - \frac{f}{\tau} \quad (1)$$

where f is the phase space density (PSD), y is the sine of the equatorial pitch angle, $y = \sin(\alpha_{eq})$, p is the momentum of the particle, and $<D_{\alpha\alpha}>$, $< D_{pp} >$, and $<D_{\alpha p}>$ are the bounce and magnetic local time averaged pitch angle, energy, and mixed components of the diffusion tensor. $T(y)$ is a function related to the

Table 1. Lower Band Chorus Wave Parameters at $L = 10$

Latitude Coverage	$\lvert\lambda\rvert < 3°$	$\lvert\lambda\rvert < 15°$	$\lvert\lambda\rvert < 40°$
Wave intensity	$\lvert\lambda\rvert < 15°$: $B_w(\lambda) = 17.94 \cdot 10^{-3.906 \cdot 10^{-2} \cdot \lvert\lambda[°]\rvert}$ [pT]		
	$\lvert\lambda\rvert > 15°$: $B_w(\lambda) = 4.66$ [pT] (assumed)		
Wave spectral properties	$\omega_m/\Omega_{ce} = 0.05$	$\omega_m/\Omega_{ce} = 5 \cdot 10^{-4}$	$\omega_m/\Omega_{ce} = 5 \cdot 10^{-4}$
	$\delta\omega/\Omega_{ce} = 0.2$	$\delta\omega/\Omega_{ce} = 0.2$	$\delta\omega/\Omega_{ce} = 0.2$
	$\omega_{lc}/\Omega_{ce} = 0.03$	$\omega_{lc}/\Omega_{ce} = 0.03$	$\omega_{lc}/\Omega_{ce} = 0.03$
	$\omega_{uc}/\Omega_{ce} = 0.5$	$\omega_{uc}/\Omega_{ce} = 0.5$	$\omega_{uc}/\Omega_{ce} = 0.5$
Wave normal	$\theta_m = 0°, \delta\theta = 30°, \theta_{lc} = 0°, \theta_{uc} = 70°$		

bounce time and it is given in *Orlova and Shprits* [2011], and τ is the electron lifetime and it equals one quarter of the bounce period inside the loss cone.

Quasilinear diffusion coefficients are calculated with the Full Diffusion Code (FDC) [*Ni et al.*, 2008; *Shprits and Ni*, 2009; *Orlova and Shprits*, 2011] using $\pm 5, \pm 4, \ldots, 0$ harmonics, and they are used as an input to the VERB code. The FDC code uses the formulation from *Glauert and Horne* [2005] and *Albert* [2005], and it is capable of calculating resonance scattering rates including Landau and cyclotron resonance scattering by obliquely propagating waves, which are solved using the change of variables suggested in *Orlova and Shprits* [2011]. The code assumes that the wave power spectral density $B^2(\omega)$ is distributed according to a Gaussian frequency distribution with median value ω_m, bandwidth $\delta\omega$, and fixed upper and lower cutoffs ω_{uc} and ω_{lc}, respectively

$$B^2(\omega) = \begin{cases} A^2 \exp\left[-\left(\frac{\omega-\omega_m}{\delta\omega}\right)^2\right] & \text{for} \quad \omega_{lc} \le \omega \le \omega_{uc} \\ 0 & \text{otherwise} \end{cases} \tag{2}$$

where the term A^2 can be written as follows [*Glauert and Horne*, 2005]

$$A^2 = \frac{2}{\sqrt{\pi}} \frac{|B_w|^2}{\delta\omega} \left[\text{erf}\left(\frac{\omega_m - \omega_{lc}}{\delta\omega}\right) + \text{erf}\left(\frac{\omega_{uc} - \omega_m}{\delta\omega}\right)\right]^{-1} \tag{3}$$

where B_w is the averaged wave amplitude. The wave normal distribution is also assumed Gaussian and given by

$$g(X) = \exp\left[-\left(\frac{X - X_m}{X_w}\right)^2\right] \tag{4}$$

where $X = \tan(\theta)$, $X_m = \tan(\theta_m)$, $X_\omega = \tan(\delta\theta)$, θ is the wave normal angle, θ_m is the peak wave normal angle, and $\delta\theta$ is a parameter describing the angular width of the distribution. θ_{lc} and θ_{uc} in Table 1 are the lower and upper cutoffs for the wave normal angle distribution, respectively.

The wave power spectral density above is determined from the most comprehensive and recently published survey of whistler mode waves at Jupiter [*Menietti et al.*, 2016] from the Plasma Wave Investigation (PWI) on board the Galileo spacecraft [*Gurnett et al.*, 1992]. The instrument consists of two orthogonal search coil magnetometers perpendicular to the spin axis as well as an electric dipole antenna. The survey from [*Menietti et al.*, 2016] provides statistics and fittings of lower ($\beta = \omega/\Omega_{ce}$ and ranges from 0.03 to 0.5, where Ω_{ce} is the electron cyclotron frequency at the equator) and upper (β from 0.5 to 0.8) band chorus waves for two latitude ranges of $|\lambda| < 3°$ and $|\lambda| < 15°$ since no wave measurements exist at higher latitudes given the nature of Galileo's orbit. The wave model excludes any wave data from moon encounters to avoid the introduction of any moon-induced effects. The two chorus bands can be clearly observed in Figure 1a obtained from the PWI instrument. The white lines denote the cyclotron frequency Ω_{ce}, $\Omega_{ce}/2$, as well as the lower hybrid frequency Ω_{LH}. Most of the emission above Ω_{LH} is whistler mode, with centers of lower and upper bands of chorus indicated. Plasma wave data are not typically narrow banded as in terrestrial chorus, and the intensity levels for upper band chorus are usually more than 1 order of magnitude lower than for lower band chorus. Figures 6 and 7 of *Menietti et al.* [2016] provide scatterplots of PWI data as well as empirical fits to the data for lower and upper band chorus waves, respectively. The FDC code uses an input Gaussian frequency spectrum to calculate diffusion coefficients, and so we have fit the wave power spectral density in Menietti's figures with a

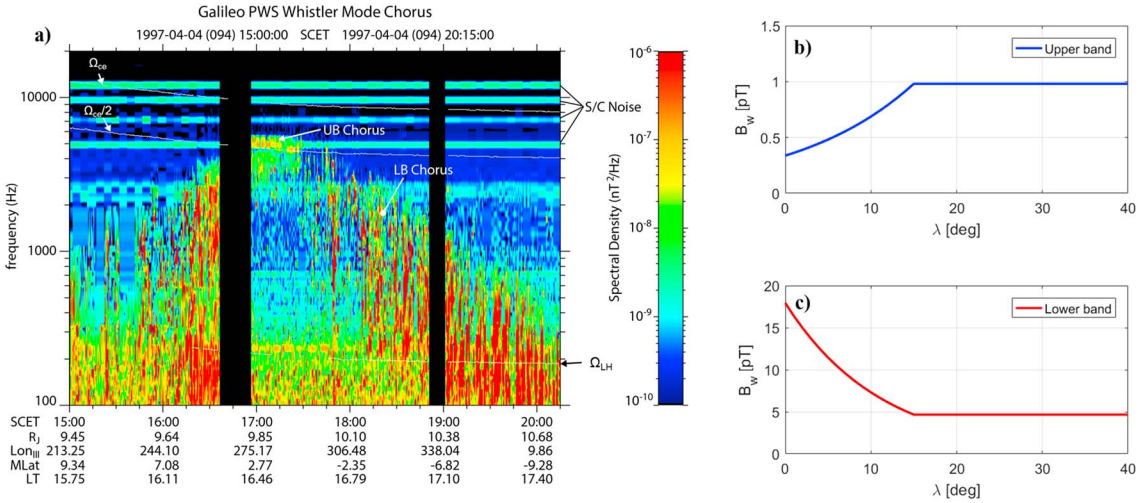

Figure 1. (a) Frequency-time spectrogram from the Plasma Wave Investigation (PWI) instrument on board Galileo. The white lines denote the cyclotron frequency Ω_{ce}, $\Omega_{ce}/2$, as well as the lower hybrid frequency Ω_{LH}. Latitudinal dependence of B_w used in the study for (b) upper and (c) lower band chorus waves.

Gaussian frequency distribution as described in equation (2). The wave normal angle is also assumed to follow a Gaussian distribution given by *Shprits et al.* [2012]. Spectral and wave normal fits used by the FDC code are summarized in Tables 1 and 2 for lower and upper band chorus, respectively.

In this investigation we want to study the effect of the latitudinal extent of the waves on electron dynamics. Figures 1b and 1c show the latitudinal dependence of B_w over a range of L shells, $10 \leq L \leq 13$, obtained from *Menietti et al.* [2016] for upper and lower band waves, respectively. The wave intensity in the figures represents an average over all local times and frequencies within the range of L shells. Galileo, however, was limited to $|\lambda| < 15°$, and so we assumed that waves capable of extending to higher latitudes would have the same intensity and spectral parameters than those for the $|\lambda| = 15°$ case. Based on this assumption, and in addition to the $|\lambda| < 3°$ and $|\lambda| < 15°$ cases, we also calculate the effect that a wave coverage of $|\lambda| < 40°$ would have on the electron dynamics so that we can compare the results from this investigation with high-latitude Juno measurements of waves and particles in the near future. In addition to spectral parameters, Tables 1 and 2 summarize wave intensities and latitude coverages used in the study for lower and upper band chorus, respectively.

The electron density is also an input to the FDC code, and it is obtained from the Divine and Garrett model [*Divine and Garrett*, 1983]. The plasma density equals 30.2 cm^{-3} as given by the model at $L = 10$. Other density models [*Bagenal et al.*, 1985; *Bagenal and Delamere*, 2011] produce very similar results to the Divine and Garrett model at $L = 10$ [*Garrett et al.*, 2015]. The latitudinal variation of the plasma density is unknown, and so in this study we have assumed that density is constant with latitude. Alternatively, in this paper we have addressed the effect of a latitudinally dependent wave coverage. A latitudinally dependent density model, however, could affect the results from this investigation, which will be the topic of future studies. We have assumed a dipole magnetic field with $B_0 = 4.28$ Gauss in the equatorial plane at the surface of the planet, which is a good

Table 2. Upper Band Chorus Wave Parameters at $L = 10$

Latitude Coverage	$\|\lambda\| < 3°$	$\|\lambda\| < 15°$	$\|\lambda\| < 40°$
Wave intensity	$\|\lambda\| < 15°$: $B_w(\lambda) = 0.337 \cdot 10^{3.093 \cdot 10^{-2} \cdot \|\lambda[°]\|}$ [pT]		
	$\|\lambda\| > 15°$: $B_w(\lambda) = 0.98$ [pT] (assumed)		
Wave spectral properties	$\omega_m/\Omega_{ce} = 5 \cdot 10^{-4}$	$\omega_m/\Omega_{ce} = 0.1$	$\omega_m/\Omega_{ce} = 0.1$
	$\delta\omega/\Omega_{ce} = 0.2$	$\delta\omega/\Omega_{ce} = 0.35$	$\delta\omega/\Omega_{ce} = 0.35$
	$\omega_{lc}/\Omega_{ce} = 0.5$	$\omega_{lc}/\Omega_{ce} = 0.5$	$\omega_{lc}/\Omega_{ce} = 0.5$
	$\omega_{uc}/\Omega_{ce} = 0.8$	$\omega_{uc}/\Omega_{ce} = 0.8$	$\omega_{uc}/\Omega_{ce} = 0.8$
Wave normal	$\theta_m = 0°, \delta\theta = 30°, \theta_{lc} = 0°, \theta_{uc} = 70°$		

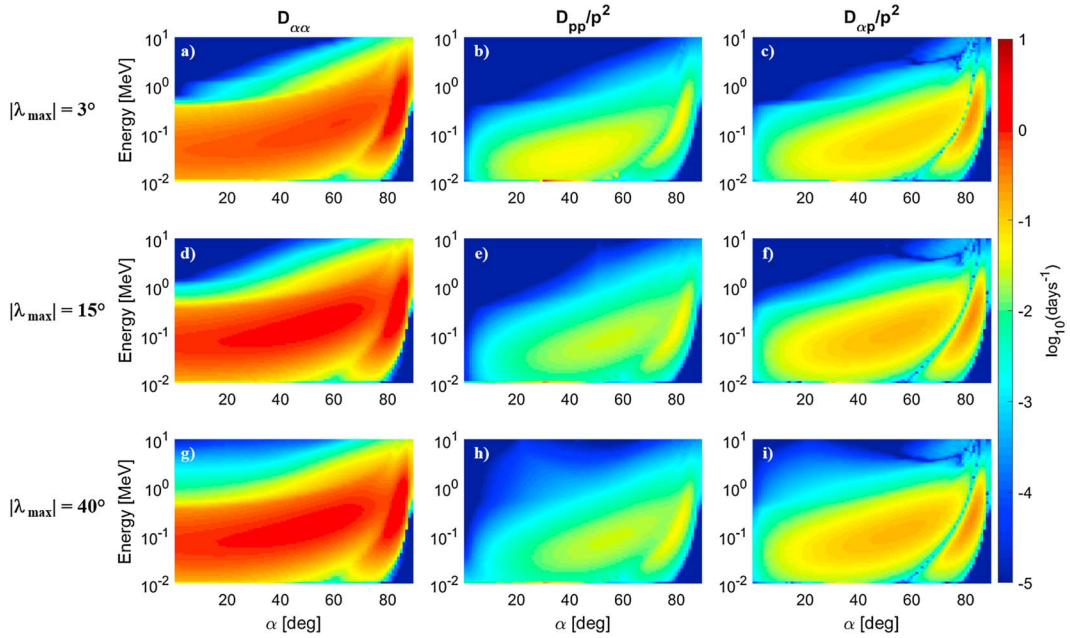

Figure 2. Diffusion coefficients calculated with the FDC code using the lower band chorus waves model in Figure 1 c. Each row corresponds to a different wave latitudinal coverage, and the three different diffusion rates (pitch angle, energy, and mixed diffusion) are given in the different columns.

approximation in the inner Jovian magnetosphere. We should also note that at $L = 10$, the contribution from Europa's induced magnetic field is negligible compared to Jupiter's background field [*Kivelson et al.*, 1999].

The empirical Galileo Interim Radiation Electron model version 2 (GIRE2) [*de Soria-Santacruz et al.*, 2016] is used to calculate the initial condition for the PSD as a function of energy $f(E)|_{GIRE2}$ at $L = 10$. The GIRE2 model is based on 10 min averages from the Energetic Particle Detector (EPD) on Galileo as well as on Pioneer and Voyager data for those regions that were poorly covered by Galileo. A sinusoidal pitch angle α dependence is assumed as given by *Albert and Young* [2005]. The initial PSD as a function of energy and pitch angle can then be expressed as follows:

$$\begin{aligned} f(E,\alpha)|_{GIRE2} &= f(E)|_{GIRE2} \sin\alpha \quad \text{for} \quad \alpha > \alpha_{lc} \\ f(E,\alpha)|_{GIRE2} &= 0 \quad \text{for} \quad \alpha \le \alpha_{lc} \end{aligned} \tag{5}$$

where $\alpha_{lc} = 1.3°$ is the equatorial loss cone at $L = 10$ assuming that particles are lost at $R_J = 1$, where R_J is the distance from the center of Jupiter in Jovian radii. With the purpose of studying the sensitivity of the interaction to the initial PSD, we also analyze the evolution of the electron distribution starting from two other initial conditions: a flat initial PSD and the analytical PSD spectrum from *Albert and Young* [2005]. The simulation results from these two assumed initial conditions are compared to the evolution of the observed initial condition $f(E,\alpha)|_{GIRE2}$ as a result of its interaction with chorus waves.

Boundary conditions in energy and pitch angle also have to be defined in the 2-D simulations. The flux at the loss cone is set to zero, while the boundary condition at $\alpha = 90°$ is set to $df/d\alpha = 0$. Similarly, the flux at both the minimum (10 keV) and maximum (10 MeV) energy boundaries is set to constant and equal to its initial value, which assumes balance between sources and losses.

3. Simulation Results of Realistic Electron-Whistler Interactions at Jupiter

Pitch angle, energy, and mixed terms diffusion coefficients are presented in Figures 2 and 3 for lower and upper band chorus waves, respectively. Each column corresponds to a diffusion coefficient, while the rows correspond to three latitudinal coverages of the waves: <3, <15, and <40° It is evident from the figures that diffusion due to lower band chorus is several orders of magnitude stronger than that from upper band chorus for most of the considered energies and pitch angles. For both bands, pitch angle diffusion rates are larger than energy rates for all energies and pitch angles. However, we need to solve the diffusion equation in order

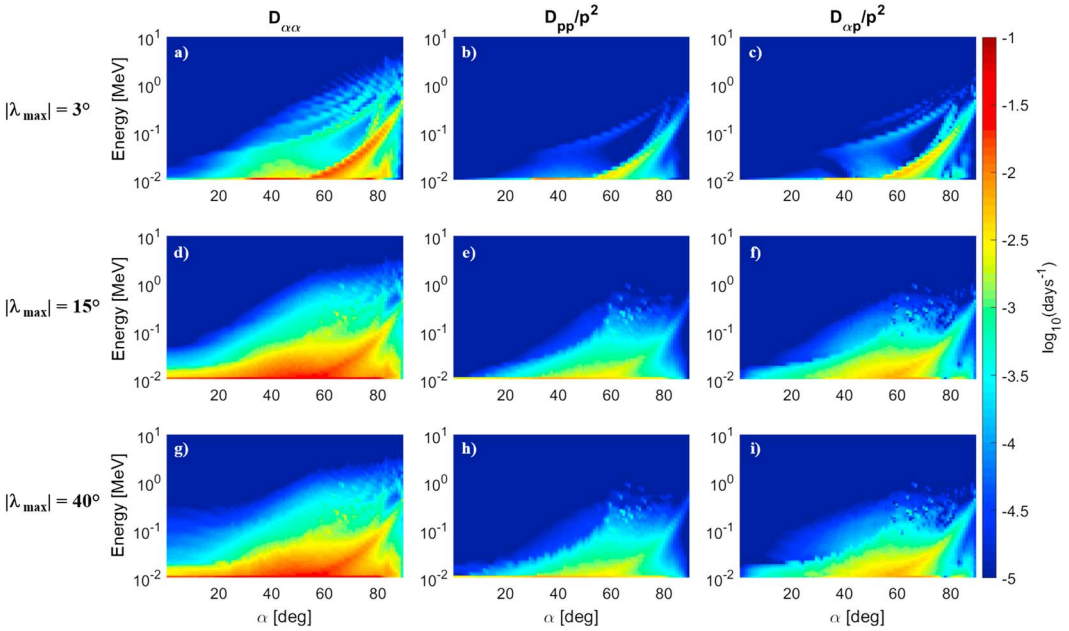

Figure 3. Same as Figure 2 but for the upper band chorus wave model in Figure 1 b).

to compare the effect of pitch angle and energy diffusion coefficients on the electron PSD. Both figures also show that increasing the latitude extent of the waves has the effect of increasing the minimum energy at which electrons are scattered near the edge of the loss cone. Scattering near the edge of the loss cone is critical as it controls the loss from the system [*Shprits et al.*, 2006b].

Figures 4–6 show the evolution of the PSD calculated with the VERB code for 100 keV, 500 keV, and 1 MeV electrons, respectively. Each column corresponds to a different initial condition described in section 2 and ploted in black: the first column is for the initial condition in *Albert and Young* [2005], the second column assumes a flat initial PSD, and the third column is for an observed initial condition based on the GIRE2 empirical model in equation (5). Similar to Figures 2 and 3, the rows correspond to the different latitudinal coverages of the waves. The PSD figures consider the combined effect of upper and lower band chorus on energetic

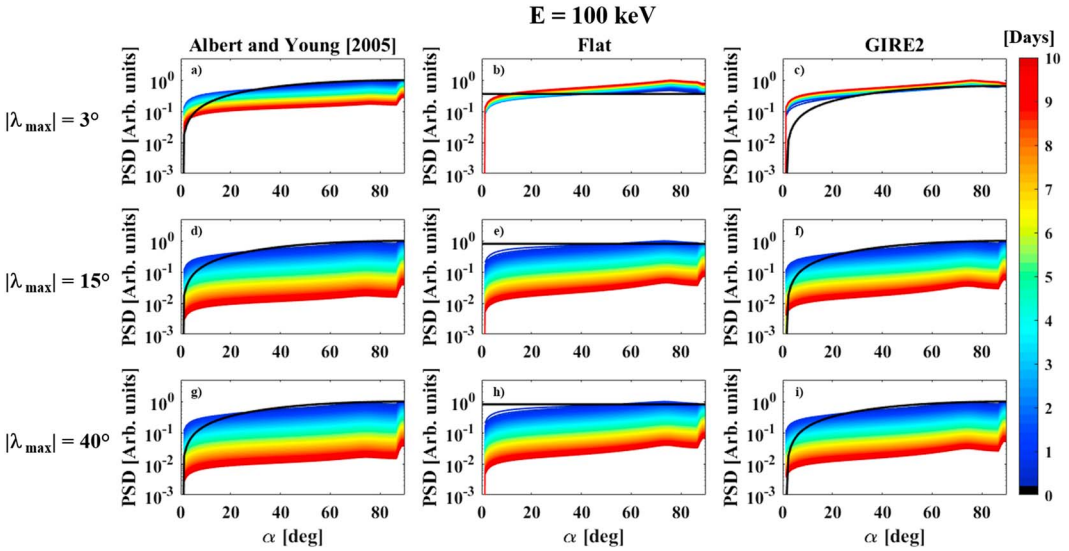

Figure 4. Evolution of the PSD calculated with the VERB code for 100 keV electrons. Each column corresponds to a different initial condition, and each row is for a different wave latitudinal coverage. The figure considers the combined effect of upper and lower band chorus on energetic electrons.

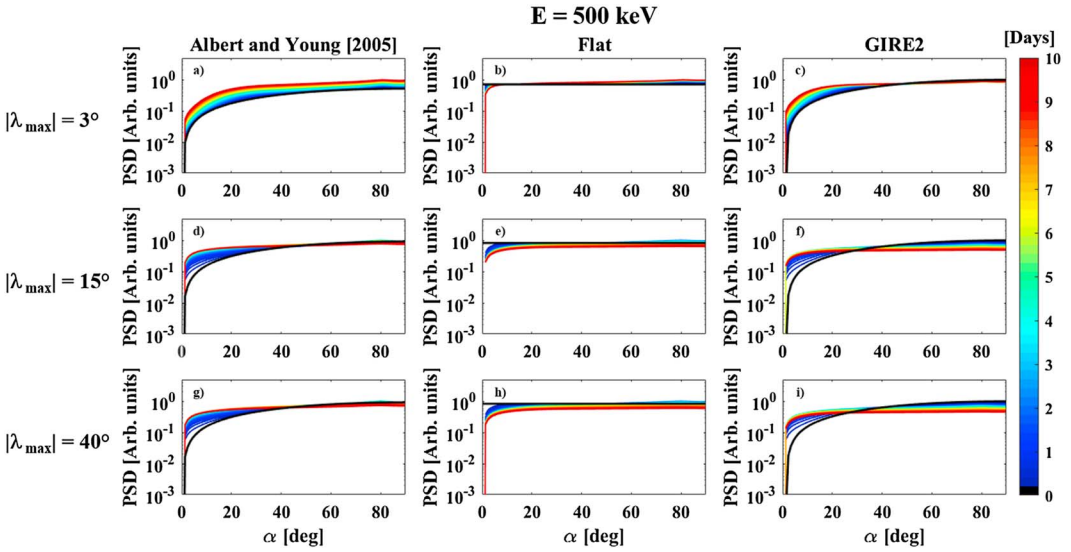

Figure 5. Same as Figure 4 but for 500 keV electrons.

electrons. However, the contribution of upper band waves is almost negligible compared to that from lower band chorus. For the 100 keV electrons in Figure 4, diffusion leads to redistribution of particles toward lower pitch angles with some particle loss for most wave coverages and initial conditions. In the case of flat and GIRE2 initial conditions with waves up to 3°, the phase space density remains practically unchanged with some minor acceleration being observed. It must be noted that the energy spectrum is always decreasing with energy and it is always steep [*de Soria-Santacruz et al.*, 2016], which means that an enhanced PSD at a fixed energy has to come from the lower energies in the spectrum. For the cases with wave coverages of 15° and 40°, particle lifetimes are less than 4 days as calculated with the method in *Shprits et al.* [2006b]. The losses in Figures 4f and 4i for the observed initial profile from GIRE2 do not mean that acceleration is not important but may indicate that additional acceleration mechanisms may have to be considered for 100 keV electrons, possibly due to radial diffusion or interchange instability-driven injections. As already noted by *Shprits et al.* [2012] and as suggested in Figure 4, the competition between loss and acceleration mechanisms can be influenced by the latitudinal distribution of the waves. For the 500 keV electrons in Figure 5, there is some redistribution of particles toward lower pitch angles, but in general we observe that chorus waves have

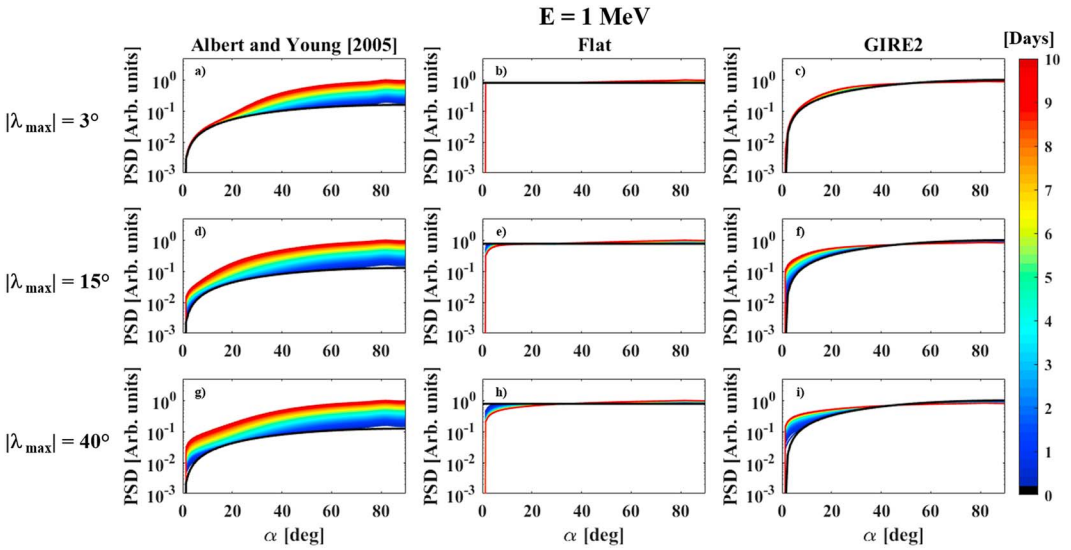

Figure 6. Same as Figure 4 but for 1 MeV electrons.

a small effect on 500 keV electrons. An exception is the case in Figure 5a (initial condition from *Albert and Young* [2005] and waves up to 3°), where there is some electron acceleration. Finally, Figure 6 presents the results for 1 MeV electrons, where we can observe intense acceleration from the *Albert and Young* [2005] initial condition that agrees with the results in *Shprits et al.* [2012]. For the flat and GIRE2 initial conditions, however, 1 MeV electrons remain practically unchanged except for a small redistribution of particles toward low pitch angles. These results are discussed in the following section.

4. Discussion and Summary

We have analyzed the effect of realistic chorus waves in the Jovian magnetosphere on the dynamics of energetic electrons at $L = 10$. We have calculated pitch angle and energy diffusion that result from the interaction with upper and lower band chorus waves obtained from the most up to date wave model based on the PWI instrument on Galileo. Previous studies of wave-particle interactions at Jupiter were based on preliminary chorus measurements [*Horne et al.*, 2008] and lacked information on spectral and spatial parameters [*Shprits et al.*, 2012; *Woodfield et al.*, 2013, 2014]. In the present study, we incorporated this information based on the extensive survey of chorus waves from *Menietti et al.* [2016]. Some characteristics of the new wave model are that it provides spectral and spatial wave distributions and that it predicts smaller wave amplitudes compared to those in previous studies. We must note that nonlinear acceleration mechanisms like Relativistic Turning Acceleration (RTA) and Ultrarelativistic Acceleration (URA) have also been proposed to explain the dynamics of energetic electrons in planetary magnetospheres. *Summers and Omura* [2007] performed simulations of individual electrons and showed that RTA and URA can accelerate them from several hundreds of keV to ultrarelativistic energies. The effects RTA or URA, however, have not been estimated in the context of global radiation belt dynamics, and future research will be needed to study if inclusion of these phenomena may improve the results of the simulations.

We have shown that diffusion coefficients from lower band chorus are several orders of magnitude stronger than those from upper band chorus for most energies and pitch angles. Moreover, the contribution to the electron dynamics from upper band waves is almost negligible compared to that from lower band chorus. We studied the evolution of the electron phase space density as a function of the wave latitudinal coverage and the initial electron distribution. The realistic wave model used in this study was limited by the latitude coverage of the Galileo spacecraft ($|\lambda| < 15°$), and so for larger latitudes (up to $|\lambda| = 40°$) we assumed that waves would have the same intensity and spectral parameters than those for the $|\lambda| = 15°$ case. As already noted by *Shprits et al.* [2012], we confirmed that the competition between loss and acceleration mechanisms can be influenced by the latitudinal distribution of the waves. For 100 keV particles, we observed that in most cases diffusion leads to redistribution of particles toward lower pitch angles with some particle loss, which seems to indicate that additional acceleration mechanisms, like radial diffusion or interchange instability-driven injections, may be missing from the simulations. For 100 keV electrons, the resulting electron distribution is clearly dependent on the latitude coverage of the waves. Moreover, the wave acceleration process, or energy diffusion, depends on the gradient of the electron phase space density with energy. The data given in the GIRE2 model is a result of averaging data from several different passes of Galileo and other spacecraft measurements. It is likely that the GIRE2 model is a better representation of the final state of the electron phase space density after the action of the waves and other transport effects. For energies above >500 keV, observed (from GIRE2) and flat initial distributions are only weakly affected by chorus waves independently of the wave coverage, which seems to indicate that pitch angle and energy diffusion alone could account for the phase space density given by the empirical GIRE2 model for >500 keV electrons, or there may be additional acceleration and loss mechanisms that balance each other. Ideally, however, one requires the initial distribution of the electron phase space density before transport takes place to assess the importance of wave acceleration, but this is not available. For example, *Woodfield et al.* [2013, 2014] show that wave-particle acceleration in the absence of electron transport can produce a radiation belt approaching that of the GIRE2 model, but the inclusion of transport effects improves the comparison with data. So although the simulations here might at first suggest that the effects of wave acceleration are limited, one must bear in mind that there is no unique solution. What is clear from the results in this study is that the shape of the electron phase space density and the latitudinal extent of the waves are important for both electron acceleration and loss. The Juno spacecraft will soon release wave and particle measurements at large latitudes, which will be used to validate the assumptions and results in this study in the near future.

Acknowledgments
The research was carried out at the Jet Propulsion Laboratory, California Institute of Technology, under a contract with the National Aeronautics and Space Administration. The University of California Los Angeles and the University of Iowa acknowledge support from a NASANNX11AM36G grant. We acknowledge Galileo PWI data obtained from the University of Iowa and available in the Planetary Data System (https://pds.nasa.gov/).

References

Albert, J. M. (2005), Evaluation of quasi-linear diffusion coefficients for whistler mode waves in a plasma with arbitrary density ratio, *J. Geophys. Res.*, *110*, A03218, doi:10.1029/2004JA010844.

Albert, J. M., and S. L. Young (2005), Multidimensional quasi-linear diffusion of radiation belt electrons, *Geophys. Res. Lett.*, *32*, L14110, doi:10.1029/2005GL023191.

Bagenal, F., and P. A. Delamere (2011), Flow of mass and energy in the magnetospheres of Jupiter and Saturn, *J. Geophys. Res.*, *116*, A05209, doi:10.1029/2010JA016294.

Bagenal, F., R. L. McNutt Jr., J. W. Belcher, H. S. Bridge, and J. D. Sullivan (1985), Revised ion temperatures for Voyager plasma measurements in the Io plasma torus, *J. Geophys. Res.*, *90*(A2), 1755–1757, doi:10.1029/JA090iA02p01755.

Berge, G. L., and S. Gulkis, (1976), Earth-based observations of Jupiter: Millimeter to meter wavelengths, Tech. Rep., Univ. of Arizona Press, Tucson, Ariz.

Bolton, S. J., et al. (2002), Ultra-relativistic electrons in Jupiter's radiation belts, *Nature*, *415*(6875), 987–991.

Burke, B. F., and K. L. Franklin (1955), Observations of a variable radio source associated with the planet Jupiter, *J. Geophys. Res.*, *60*(2), 213–217.

Carr, T. D., and S. Gulkis (1969), The magnetosphere of Jupiter, *Annu. Rev. Astron. Astrophys.*, *7*, 577–618.

De Pater, I. (1981), Comparison of the radio data and model calculations of Jupiter's synchrotron radiation, 1. The high energy electron distribution in Jupiter's inner magnetosphere, *J. Geophys. Res.*, *86*(A5), 3397–3422.

De Pater, I., and C. K. Goertz (1990), Radial diffusion models of energetic electrons and Jupiter's synchrotron radiation: 1. Steady state solution, *J. Geophys. Res.*, *95*(A1), 39–50.

De Pater, I., and C. Goertz (1994), Radial diffusion models of energetic electrons and Jupiter's synchrotron radiation: 2. Time variability, *J. Geophys. Res.*, *99*(A2), 2271–2287.

de Soria-Santacruz, M., H. B. Garrett, R. W. Evans, I. Jun, W. Kim, C. Paranicas, and A. Drozdov (2016), An empirical model of the high-energy electron environment at Jupiter, *J. Geophys. Res. Space Physics*, *121*, 9732–9743, doi:10.1002/2016JA023059.

Divine, N., and H. B. Garrett (1983), Charged particle distributions in Jupiter's magnetosphere, *J. Geophys. Res.*, *88*(A9), 6889–6903, doi:10.1029/JA088iA09p06889.

Drake, F. D., and S. Hvatum (1959), Non-thermal microwave radiation from Jupiter, *Astron. J.*, *64*, 329–330.

Dulk, G. A., Y. Leblanc, R. J. Sault, S. J. Bolton, J. H. Waite, and J. Connerney (1999a), Jupiter's magnetic field as revealed by the synchrotron radiation belts. I. Comparison of a 3-D reconstruction with models of the field, *Astron. Astrophys.*, *347*, 1029–1038.

Dulk, G. A., Y. Leblanc, R. J. Sault, and S. J. Bolton (1999b), Jupiter's magnetic field as revealed by the synchrotron radiation belts. II. Change of the 2-D brightness distribution with D_E, *Astron. Astrophys.*, *347*, 1039–1045.

Garrett, H. B., I. Jun, M. J. Ratliff, R. W. Evans, G. A. Clough, and R. W. McEntire (2002), *Galileo Interim Radiation Model*, JPL Pubication 03-006, Jet Propul. Lab., Pasadena, Calif.

Garrett, H. B., S. M. Levin, S. J. Bolton, R. W. Evans, and B. Bhattacharya (2005), A revised model of Jupiter's inner electron belts: Updating the Divine radiation model, *Geophys. Res. Lett.*, *32*, L04104, doi:10.1029/2004GL021986.

Garrett, H. B., W. Kim, and B. Belland (2015), *Jovian Plasma Environment for Mission Design*, JPL Publication 15–11, Jet Propul. Lab., California Inst. of Technol., Pasadena, Calif.

Gerard, E. (1970), Observations of Jupiter at 11.13 cm, *Astron. Astrophys.*, *8*, 181–188.

Gerard, E. (1976), Variation of the radio emission of Jupiter at 21.3 and 6.2 cm wavelength, *Astron. Astrophys.*, *50*, 353–360.

Glauert, S. A., and R. B. Horne (2005), Calculation of pitch angle and energy diffusion coefficients with the PADIE code, *J. Geophys. Res.*, *110*, A04206, doi:10.1029/2004JA010851.

Gurnett, D. A., W. S. Kurth, R. R. Shaw, A. Roux, R. Gendrin, C. F. Kennel, F. L. Scarf, and S. D. Shawhan (1992), The Galileo plasma wave investigation, *Space Sci. Rev.*, *60*(1–4), 341–355, doi:10.1007/BF00216861.

Horne, R. B., and R. M. Thorne (1998), Potential waves for relativistic electron scattering and stochastic acceleration during magnetic storms, *Geophys. Res. Lett.*, *25*(15), 3011–3014.

Horne, R. B., R. M. Thorne, S. A. Glauert, J. D. Menietti, Y. Y. Shprits, and D. A. Gurnett (2008), Gyro-resonant electron acceleration at Jupiter, *Nat. Phys.*, *4*(4), 301–304.

Jet Propulsion Laboratory, California Institute of Technology (2017), The Europa Clipper Mission. [Available at https://www.jpl.nasa.gov/missions/europa-clipper/.]

Kellogg, P. J. (1959), Van Allen radiation of solar origin, *Nature*, *183*, 1295–1297.

Kivelson, M. G., K. K. Khurana, D. J. Stevenson, L. Bennett, S. Joy, C. T. Russell, R. J. Walker, C. Zimmer, and C. Polanskey (1999), Europa and Callisto: Induced or intrinsic fields in a periodically varying plasma environment, *J. Geophys. Res.*, *104*(A3), 4609–4625, doi:10.1029/1998JA900095.

Klein, M. J. (1976), The variability of the total flux density and polarization of Jupiter's decimetric radio emission, *J. Geophys. Res.*, *81*(19), 3380–3382.

Klein, M. J., T. J. Thompson, and S. J. Bolton (1989), Systematic observations and correlation studies of variations in the synchrotron radio emission from Jupiter, in *Time Variable Phenomena in The Jovian System, NASA Spec. Publ.*, vol. 494, edited by M. J. S. Belton, R. A. West, and J. Rahe, pp. 151–155, NASA, Washington, D. C.

Menietti, J. D., R. B. Horne, D. A. Gurnett, G. B. Hospodarsky, C. W. Piker, and J. B. Groene (2008), A survey of Galileo Plasma Wave Instrument observations of Jovian whistler-mode chorus, *Ann. Geophys.*, *26*, 1819–1828.

Menietti, J. D., J. B. Groene, T. F. Averkamp, R. B. Horne, E. E. Woodfield, Y. Y. Shprits, M. de Soria-Santacruz Pich, and D. A. Gurnett (2016), Survey of whistler mode chorus intensity at Jupiter, *J. Geophys. Res. Space Physics*, *121*, 9758–9770, doi:10.1002/2016JA022969.

Ni, B., R. M. Thorne, Y. Y. Shprits, and J. Bortnik (2008), Resonant scattering of plasma sheet electrons by whistler-mode chorus: Contribution to diffuse auroral precipitation, *Geophys. Res. Lett.*, *35*, L11106, doi:10.1029/2008GL034032.

Orlova, K. G., and Y. Y. Shprits (2011), On the bounce-averaging of scattering rates and the calculation of bounce period, *Phys. Plasmas*, *18*(9), 092904, doi:10.1063/1.3638137.

Radhakrishnan, V., and J. A. Roberts (1960), Polarization and angular extent of the 960-Mc/sec radiation from Jupiter, *Phys. Rev. Lett.*, *4*(10), 493.

Santos-Costa, D., and S. A. Bourdarie (2001), Modeling the inner Jovian electron radiation belt including non-equatorial particles, *Planet. Space Sci.*, *49*(3), 303–312.

Santos-Costa, D., S. J. Bolton, R. M. Thorne, Y. Miyoshi, and S. M. Levin (2008), Investigating the origins of the Jovian decimetric emission's variability, *J. Geophys. Res.*, *113*, A01204, doi:10.1029/2007JA012396.

Schulz, M., and L. J. Lanzerotti (1972), *Particle Diffusion in the Radiation Belts*, Springer, New York.

Shprits, Y. Y., and B. Ni (2009), Dependence of the quasi-linear scattering rates on the wave normal distribution of chorus waves, *J. Geophys. Res.*, *114*, A11205, doi:10.1029/2009JA014223.

Shprits, Y. Y., and R. M. Thorne (2004), Time dependent radial diffusion modeling of relativistic electrons with realistic loss rates, *Geophys. Res. Lett.*, *31*, L08805, doi:10.1029/2004GL019591.

Shprits, Y. Y., R. M. Thorne, R. B. Horne, S. A. Glauert, M. Cartwright, C. T. Russell, D. N. Baker, and S. G. Kanekal (2006a), Acceleration mechanism responsible for the formation of the new radiation belt during the 2003 Halloween solar storm, *Geophys. Res. Lett.*, *33*, L05104, doi:10.1029/2005GL024256.

Shprits, Y. Y., W. Li, and R. M. Thorne (2006b), Controlling effect of the pitch angle scattering rates near the edge of the loss cone on electron lifetimes, *J. Geophys. Res.*, *111*, A12206, doi:10.1029/2006JA011758.

Shprits, Y. Y., D. Subbotin, and B. Ni (2009), Evolution of electron fluxes in the outer radiation belt computed with the VERB code, *J. Geophys. Res.*, *114*, A11209, doi:10.1029/2008JA013784.

Shprits, Y. Y., J. D. Menietti, X. Gu, K. Kim, and R. B. Horne (2012), Gyroresonant interactions between the radiation belt electrons and whistler mode chorus waves in the radiation environments of Earth, Jupiter, and Saturn: A comparative study, *J. Geophys. Res.*, *117*, A11216, doi:10.1029/2012JA018031.

Sicard, A., and S. Bourdarie (2004), Physical Electron Belt Model from Jupiter's surface to the orbit of Europa, *J. Geophys. Res.*, *109*, A02216, doi:10.1029/2003JA010203.

Sicard-Piet, A., S. Bourdarie, and N. Krupp (2011), JOSE: A new Jovian specification environment model, *IEEE Trans. Nucl. Sci.*, *58*(3), 923–931.

Subbotin, D., Y. Shprits, and B. Ni (2010), Three-dimensional VERB radiation belt simulations including mixed diffusion, *J. Geophys. Res.*, *115*, A03205, doi:10.1029/2009JA015070.

Summers, D., and Y. Omura (2007), Ultra-relativistic acceleration of electrons in planetary magnetospheres, *Geophys. Res. Lett.*, *34*, L24205, doi:10.1029/2007GL032226.

Summers, D., R. M. Thorne, and F. Xiao (1998), Relativistic theory of wave-particle resonant diffusion with application to electron acceleration in the magnetosphere, *J. Geophys. Res.*, *103*(A9), 20,487–20,500.

Williams, D. J., R. W. McEntire, S. Jaskulek, and B. Wilken (1992), The Galileo energetic particles detector, *Space Sci. Rev.*, *60*(1–4), 385–412, doi:10.1007/BF00216863.

Woodfield, E. E., R. B. Horne, S. A. Glauert, J. D. Menietti, and Y. Y. Shprits (2013), Electron acceleration at Jupiter: Input from cyclotron-resonant interaction with whistler-mode chorus waves, *Ann. Geophys.*, *31*, 1619–1630.

Woodfield, E. E., R. B. Horne, S. A. Glauert, J. D. Menietti, and Y. Y. Shprits (2014), The origin of Jupiter's outer radiation belt, *J. Geophys. Res. Space Physics*, *119*, 3490–3502, doi:10.1002/2014JA019891.